Utility of chemiluminescence monitoring for active control of combustion

L. Zimmer, S. Tachibana
Japan Aerospace Exploration Agency (JAXA)
7-44-1 Jindaiji-Higashi, Chofu, Tokyo, 182-8522 Japan
E-mail:zimmer.laurent@jaxa.jp

Abstract

The purpose of this article is to evaluate the chemiluminescence advantages in an active control strategy for lean premixed low NOx gas turbines. Measuring simultaneously three different wavelengths (OH*, CH* and background emission) gives an estimation of the actual stoichiometry within the combustor. The typical temporal resolution remains limited to the order of 0.2s for an accurate measurement but the sensitivity is quite high for stoichiometry lower than 0.5, which is the main target of low NOx combustor. Using high sampling rate (10kHz) allows looking at the frequency domain of the chemiluminescence. It is shown that peaks appear at the same frequencies than the pressure signal. Traversing the chemiluminescence probe versus the pressure probe allows determining the typical nature of the oscillations. Using phase-locked chemiluminescence images provides dynamic information of the oscillations. It is shown that for strong oscillations, the flame is influenced by a vortex-like structure issued from the supply pipes, whereas low oscillations do not show such phenomena. The cases of good control and bad control are also discussed with simultaneous measurements of pressure and heat release. It is shown that good control reduced the pressure fluctuations as well as generates a more uniform heat release in time. The coupling of pressure and heat release can be used to predict the appearance of strong oscillations due to a coupling between the two. Finally, using temporally resolved chemiluminescence, the effect of secondary injection systems can be described and using this as an input in simple models allows predicting the best control strategies, as far as frequency, opening time and time delay versus pressure are concerned. Comparisons with actual experiments are reported and similar behavior is found between the model and the experiments.

1. Introduction

Efforts are being made in the world to reduce pollutant emission from gas turbines. One attractive way is the lean premixed combustion that offers lower flame temperature and therefore reduces the thermal NOx creation. However, having a combustor that can operate in stable condition with a wide operating range is still a challenge and oscillations are likely to occur for some conditions. Those instabilities may be important enough to have pressure waves that can damage the internal structure of the combustor or leading to blow out of the flame. It is of practical interest to have robust active control of combustion. One of the aspects in an active control loop is the sensing technique. For purely aero-acoustics problems, pressure sensors are well suited (Anthoine *et al.* 2003) and a typical actuator may be a loudspeaker. However combustion involves also heat release and chemical reactions and it seems possible to take benefit from this aspect to include other sensing and actuating devices.
Due to the harsh environment inside a combustor, intrusive techniques (such as gas sampling) may not be an adequate choice in control loop strategies, as their temporal reliability may not be very high. Despite these considerations, it may be useful in some small-scales turbines for developing active control strategies (Wachsman *et al.* 2004). Non-intrusive techniques may however require an external input (such as the case for DLAS techniques as presented in (Sanders *et al.* 2002) which requires a laser at high repetition rate for diagnostics). This solution may not be adequate for long time use in gas turbines and one may look towards chemiluminescence as being a good candidate for sensing purpose.
Therefore, this paper examines the utility of chemiluminescence measurements for active control of combustion. The first part deals with the operating point control, which typically is a low frequency control loop. The second part shows that simultaneous measurements of pressure and chemiluminescence give a better insight in the nature of the oscillating modes. The third part shows that for real time analysis, coupling pressure to chemiluminescence increases the reliability and dynamics of oscillating combustion detections. The fourth part will show that chemiluminescent measurements as input for models give a good idea of the best choices for active control as for injection rate and time delays are concerned. Finally, the occurrence of blow out is discussed and typical examples are shown.

2. Operating point control

To have a minimum of pollutant emission as well as a safe margin compared to blow off or oscillating combustion, the exact equivalence ratio should be known at any time. However, in gas turbines, the exact amount of air supplied is not precisely known and variations in the fuel properties may also affect the actual stoichiometry. Therefore, it is of practical importance to have a real time monitoring of this quantity. However, gas turbines are harsh environment and therefore, non-intrusive techniques are preferable. Some studies have shown that it may be possible to record incoming equivalence ratio using absorption techniques (Lee *et*

al.,2000). However, again problems may come from long terms use of laser source and the influence of oscillations may not be negligible. Therefore, chemiluminescence was chosen but whereas many studies reported before (Docquier *et al.*, 2002), (Lee and Santavicca, 2003) used spectrometer (low time resolution); the present sensing device can have higher temporal measurements. For this study, a lean pre-heated premixed swirl-stabilized methane-air flame is first used. The swirl number is 0.23 and the preheated temperature can reach 600K at the inlet of the test section. Typical inlet velocities were ranging from 10 to 20 $m.s^{-1}$.Further details may be found in a previous paper (Zimmer *et al.*, 2003).

Chemiluminescence is measured through a double condenser lens of 300mm of focal length. The light exiting the lens is sent, through an optic fiber to a specbox (Hamamatsu, Inc.). This divides afterwards, through a series of band-pass filter and mirrors to four different photo-multipliers. The optical properties of each band-pass filters as well as the radical measured are shown in Table 1. It is worth noting that the two last wavelengths are representing the background emission in lean premixed flames, as it has been shown that C_2 radicals can hardly be detected for typical stoichiometry below 0.9. The measurement is resulting from the integration over a volume and therefore no fine spatial resolution can be obtained.

	PM1	PM2	PM3
Wavelength (nm)	308±10	431±2	473±2
Radicals	OH*	CH*	C_2* / CO_2*

Table 1 Optical properties of the specbox

It has been shown in Zimmer *et al*, 2003 that monitoring the ratio of (OH*-background) / (CH* - background) lead to an indication of the actual stoichiometry. To validate the presented approach (use of 3 different PMT rather than one spectrometer for a considerable gain in the frequency domain), measurements are also performed inside the target combustor. It is a swirl-type stabilized flame, having 12 vanes of 30° of angle each. The dimensions of the combustor are 100x100mm for the section and a total length of 210mm, extensible to 810mm to change the acoustic frequencies. An important feature is the presence of secondary injection orifices that may be used for active control strategies. A more complete description can be found in (Tachibana *et al.*, 2004). The calibration is done without injecting the secondary fuel, considering only premixed methane-air flames. The location of the lens is at 20mm from the exit of the swirl, along the centerline of the combustor. Typical variable are inlet temperature and inlet velocity. Calibration was performed for a velocity of $30m.s^{-1}$, pre heated at 700K. One can notice on Figure 1 that the initial slope (for equivalence ratio (E.R.) below 0.5) is very steep, meaning that small changes in the stoichiometry leads to strong changes in the ratio between OH* and CH*. The background is removed on both signals (using PM3). The results presented here are mean results obtained over 10s.

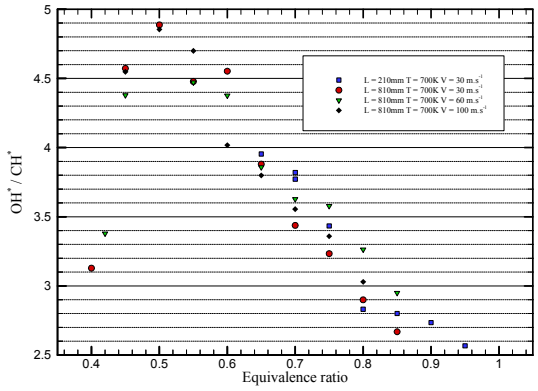

Figure 1 Chemiluminescent ratios in demonstration combustor

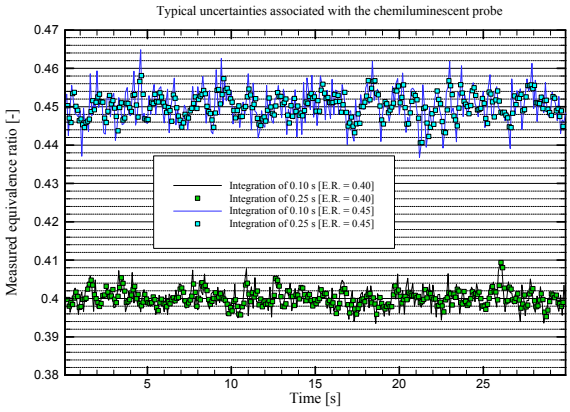

Figure 2 Time series evaluation of stoichiometry

This is very interesting as the lean blowout limit lies within 0.4 and 0.45 depending on the velocity chosen. One can notice that the length of the combustor, affecting strongly the inner acoustics has no influence on the ratio. Of course the actual ratio is non-monotonic, as already shown in the previous section dealing with a small-scale combustor. However, in the region where blowout may occur (less than 0.5), the shape is monotonic, leading to non-ambiguous results. The next task consists in determining the typical temporal response and accuracy of this measurement. The bulk velocity is set to $30m.s^{-1}$, pre-heated at 700K. The value of the blowout is 0.38 for this case. This is illustrated in Figure 2, where two sampling rates are considered (10Hz and 4Hz). The imposed equivalence ratio is respectively 0.40 and 0.45. One can notice that the measured equivalence ratio (inferred from measured chemiluminescence ratio) is in good accordance with respect to the imposed one. Measuring the typical deviations as function of the sampling frequency gives an idea of the uncertainties. The results are displayed in Table 2 where windows from 0.1 to 0.5s are considered for three different stoichiometry. One can

Windows	0.10	0.20	0.30	0.40	0.50
0.40	0.0031	0.0022	0.0018	0.0016	0.0014
0.45	0.0172	0.0125	0.0102	0.0089	0.0081
0.50	0.0122	0.0085	0.0068	0.0060	0.0055

Table 2 Typical uncertainties for lean flames

see that taking windows of 0.1 to measure the equivalence ratio through chemiluminescence ratio gives raise to typical uncertainties of the order of 0.01 to 0.02 (which may represent 4%). The highest errors are found for equivalence ratio around 0.45, because it has been shown that the OH*/CH* is very sensitive in this region. Using lower sampling frequency (5Hz or 3.33Hz) enables to reduce drastically the uncertainties to levels below 3% for the different cases shown here.

In this section, is has been shown that taking the ratio of chemiluminescent species can yield the information concerning the burning equivalence ratio. This information may be used for low frequency (of the order of a few Hertz) loop control of the operating point. The main difference with previously published paper is that high frequency acquisition is also possible using this probe and the next section deals with this subsequent advantage compared to spectrometer with lower temporal possibilities.

3. Chemiluminescence for understanding oscillating combustion

3.1 Frequency domain

Another important aspect of chemiluminescence is that time series data are easily obtained, in opposite to PLIF techniques. As it is a non-intrusive technique, it is also easy to modify the measurement points and therefore verify the type of instabilities (axial, tangential or radial). To understand oscillating combustion, the target combustor is used and a pressure transducer (Kulite Semiconductor Products, Inc., Model XTL-190-15G) is located in the center plane at a distance of 20mm from the exit of the swirl.

Both pressure and CH* emission are acquired at 10 kHz (via OnoSokki, DS-200, Graduo). The lens is mounted on a traverse system, so that the measurement volume can be easily changed during the experiments. If not stated explicitly, all measurements of CH* are done perpendicular to the pressure probe. In case of oscillations, the pressure and the heat release are in phase, as the maximum of correlation is measured for a time delay equals to 0ms when the lens is perpendicular to the pressure probe. When moving the chemiluminescence probe in the stream wise direction (see Figure 3), one can see that for positions closer to the exit of the swirl (X=-10mm), CH* is in advance of 0.42ms compared to measurements done at the location of the pressure probe. The same time delay is observed but with an opposite sign when moving the lens further downstream. The differences in correlation mean that a wave is really traveling along the combustor.

Comparison of Power Spectrum Density between pressure and CH* is shown on Figure 4. One can notice that sometimes only acoustics oscillations are measured without noticeable effects on heat release as shown with E.R. = 0.60. This type of oscillating mode is better controlled with a loud speaker, acting directly on the acoustic field than with a modulation of heat release via secondary injection as the heat pattern does not present any sensible periodic movement. However, the pressure amplitudes associated to those instabilities remain limited and do not present serious problems for the safety of the combustor.

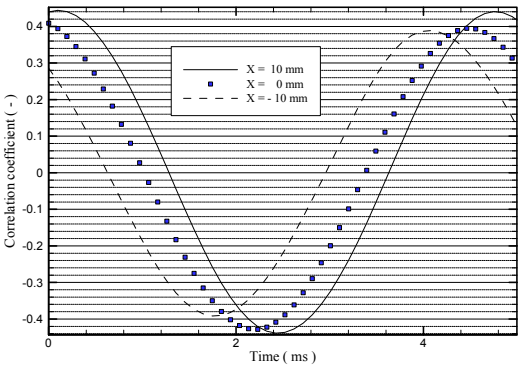

Figure 3 Correlation between pressure and CH*

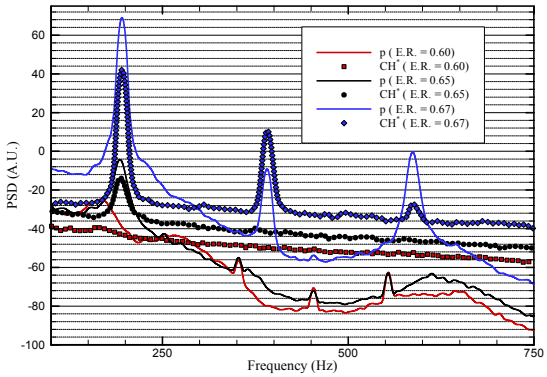

Figure 4 PSD for pressure and heat release

Increasing stoichiometry (ϕ = 0.65), one can see a peak also appearing in the chemiluminescent signal, meaning that the heat release is affected by the acoustics oscillations. This peak has the same frequency as the one obtained with pressure measurements Further increase in the oscillations result in appearance of harmonic peaks, due to a deviation from sinusoidal shape. It is worth noting that the peak associated to the three quarter wavelength rule is stronger than the harmonic of the quarter wavelength rule for pressure signal. However, this tendency cannot be seen in CH*, meaning that again, the physical basis is acoustical mode of excitation and that only the first mode does affect the fuel injection system, as being the most energetic.

This type of information can only be obtained by simultaneous measurements of pressure and chemiluminescence. The next paragraph shows the effect of the different oscillating mode on the mean flame

shape by making phase-locked chemiluminescence emission for different cases.

3.2 Phase-locked visualization

To better understand the mechanisms of oscillating combustion, phase-locked images of chemiluminescent emissions in case of oscillations are recorded. The pressure transducer is located at X = 20mm and Y = 0mm. The global chemiluminescence of OH* is recorded as function of the phase delay with respect to the pressure signal. For that purpose, an ICCD (Princeton Instruments 576G/1) is used to capture the images of PLIF, with an UV-Nikkor 105mm/f4.5 lens. Its resolution is 576 by 384 pixels and typical measured area were 75mmx50mm, which gives a magnification 0.13 mm^2/pixel. It is used in gate mode with an exposure of 40µs and an f-number of 4.5. Typically 80 images are recorded at each phase angle (20 points in case of oscillating flames, 10 points otherwise). The phase is determined with respect to the zero-crossing event in the filtered pressure signal with a positive slope. An illustration of the different phases is given in Figure 5 as well as a typical pressure signal within the combustor.

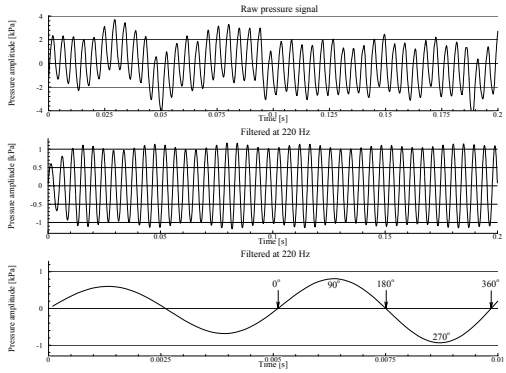

Figure 5 Raw and filtered pressure signal

	Figure 6	Figure 7	Figure 8	Figure 9
Equivalence ratio (ϕ)	0.73	0.87	0.73	0.87
Pilot (%)	0	10	0	10
Delay (ms)	0	2.4	0	0.4
Pressure [kPa]	1.83	1.83	0.80	0.56

Table 3 Experimental conditions of the phase-locked imag

The flow comes from left to right (see Figure 6-9) and the bulk velocity of 12$m.s^{-1}$ for an inlet temperature of 500K, the length of the combustor being 810mm; the typical frequencies are around 220Hz. The overall equivalence ratio for the case in Figure 6 is 0.73 (see Table 3 for full details) for a fully premixed case. Background is removed from all images and levels lower than 1% of the maximum are removed also for clarity reason. The images correspond to volume integration as no Abel transform is applied. One can notice an influence on the flame shape as a function of pressure phase.

For a phase delay of 10 °, the flame front close to the exit seems to be deformed by a vortex-like structure coming from the inside of supplying mixture. For a phase of 45 °, this behavior is emphasized with the same structure being detected. For a phase of 90 °, which represents the time where the pressure is at its maximum for a position of X=20mm along the centerline, the overall chemiluminescent emission increases. This increase is also seen for a phase delay of 125 °, but at the position of the pressure probe (which is the line over which the chemiluminescent lens is integrated), one can notice that the emission diminishes. At this time, the outer part of the flame seems to be deformed whereas the central parts (for radial positions lower than 20mm) have a flat profile. For delays between 125 ° and 205 °, one can notice that the boundaries as seen by the chemiluminescence seems to be moving with the mean flow, as typically low levels only can be found for temporal positions around 205 ° and 245 °. The fact that no signal appears for a delay of 285 ° does not mean that the flame is completely lifted up or blown out, simply that the levels may be very small compared to background emission. What is more surprising are the results for delays after 300 °, where a flame front is seen close to the exit of the swirl. It would have been more logical to see a flame front coming from the right side of the combustor (as for instance explained in Taupin *et al.*, 2002). Afterwards, this initial flame front develops and a vortex-like structure can be detected, as already mentioned for initial delays. To better understand the dynamic of the flame, simultaneous measurements with PIV are planed.

Somehow similar results can be found in case of secondary injection leading also to oscillating combustion (see Figure 7). The premixed remains unchanged but 10% of methane compared to the premixture is added and injected through small holes (1.4mm), placed inside the combustor (see Tachibana *et al.*, 2004). The overall equivalence ratio is in this case 0.87. Therefore, the overall chemiluminescence emission is higher for this case than the previous one. The secondary fuel is injected at 245Hz, with an opening time of 1.6s and a phase delay of 190 ° compared to the pressure signal, as shown in Table 3.The same mechanisms are present, even though the flame is vanishing out of the measurement region. This may comes from higher equivalence ratio (hence higher signal to noise ratio). As can be seen for a phase delay of 250 °, the central part exhibit chemiluminescent emission. This is an effect of secondary injection. This case leading to oscillations was a case for which the time delay between secondary injection and pressure was 2ms. Having a time lag of 72ms, this makes 74ms, resulting in a true phase shift of 160 °, with an opening of 1.6ms, representing 65 °. Another important phenomenon is the

interaction of the flame with a vortex. One can see that the flame shape is flat for a phase angle of 325 ° . For a phase angle of 360 ° , one can see that a vortex shape issued from the outer part of the swirl vanes (Y=25mm) modifies the primary shape. This kind of events does not appear in case of stable combustion conditions, as shown in Figure 8 and 9. One can notice that the flame shape remains similar independently of the phase delay versus pressure signal. The fluctuations of pressure remained limited to 0.8 kPa (premixed) and 0.56 kPa (partially premixed) respectively whereas the previous cases had oscillations of the order of 1.8kPa. The case exhibited in Figure 8 corresponds to a successful active control situation. The secondary injection was issued when the primary flame was lifted up, leading to no interaction between the two flames and therefore no control could be obtained.

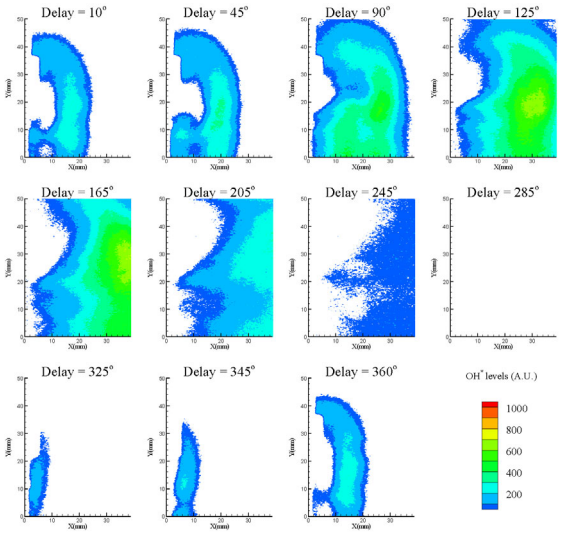

Figure 6 Premixed oscillating flame (ϕ=0.73)

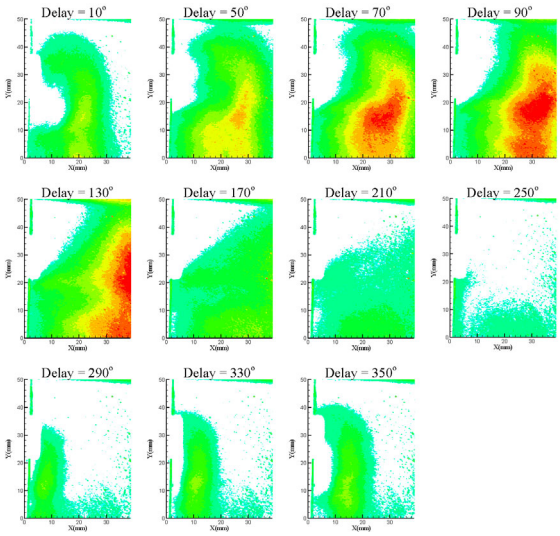

Figure 7 Partially premixed flame (ϕ=0.87)

For a phase delay of 10 ° , the flame front close to the exit seems to be deformed by a vortex-like structure coming from the inside of supplying mixture. For a phase of 45 ° , this behavior is emphasized with the same structure being detected. For a phase of 90 ° , which represents the time where the pressure is at its maximum for a position of X=20mm along the centerline, the overall chemiluminescent emission increases. This increase is also seen for a phase delay of 125 ° , but at the position of the pressure probe (which is the line over which the chemiluminescent lens is integrated), one can notice that the emission diminishes. At this time, the outer part of the flame seems to be deformed whereas the central parts (for radial positions lower than 20mm) have a flat profile. For delays between 125 ° and 205 ° , one can notice that the boundaries as seen by the chemiluminescence seems to be moving with the mean flow, as typically low levels only can be found for temporal positions around 205 ° and 245 ° . The fact that no signal appears for a delay of 285 ° does not mean that the flame is completely lifted up or blown out, simply that the levels may be very small compared to background emission. What is more surprising are the results for delays after 300 ° , where a flame front is seen close to the exit of the swirl. It would have been more logical to see a flame front coming from the right side of the combustor (as for instance explained in Taupin *et al.*, 2002). Afterwards, this initial flame front develops and a vortex-like structure can be detected, as already mentioned for initial delays. To better understand the dynamic of the flame, simultaneous measurements with PIV are planed.

Somehow similar results can be found in case of secondary injection leading also to oscillating combustion (see Figure 7). The premixed remains unchanged but 10% of methane compared to the premixture is added and injected through small holes (1.4mm), placed inside the combustor (see Tachibana *et al.*, 2004). The overall equivalence ratio is in this case 0.87. Therefore, the overall chemiluminescence emission is higher for this case than the previous one. The secondary fuel is injected at 245Hz, with an opening time of 1.6s and a phase delay of 190 ° compared to the pressure signal, as shown in Table 3.The same mechanisms are present, even though the flame is vanishing out of the measurement region. This may comes from higher equivalence ratio (hence higher signal to noise ratio). As can be seen for a phase delay of 250 ° , the central part exhibit chemiluminescent emission. This is an effect of secondary injection. This case leading to oscillations was a case for which the time delay between secondary injection and pressure was 2ms. Having a time lag of 72ms, this makes 74ms, resulting in a true phase shift of 160 ° , with an opening of 1.6ms, representing 65 ° . Another important phenomenon is the interaction of the flame with a vortex. One can see that the flame shape is flat for a phase angle of 325 ° . For a phase angle of 360 ° , one can see that a vortex shape issued from the outer part of the swirl vanes (Y=25mm) modifies the primary shape. This kind of events does not appear in case of stable combustion conditions, as

shown in Figure 8 and 9. One can notice that the flame shape remains similar independently of the phase delay versus pressure signal. The fluctuations of pressure remained limited to 0.8 kPa (premixed) and 0.56 kPa (partially premixed) respectively whereas the previous cases had oscillations of the order of 1.8kPa. The case exhibited in Figure 8 corresponds to a successful active control situation. The secondary injection was issued when the primary flame was lifted up, leading to no interaction between the two flames and therefore no control could be obtained.

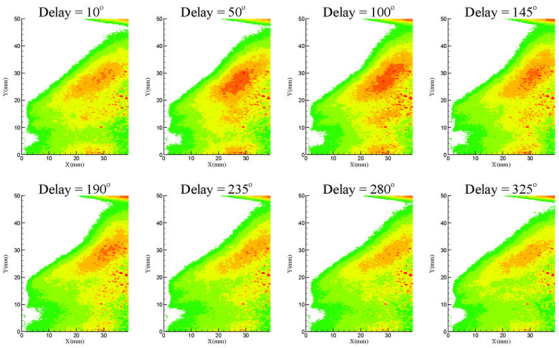

Figure 8 Premixed stable flame

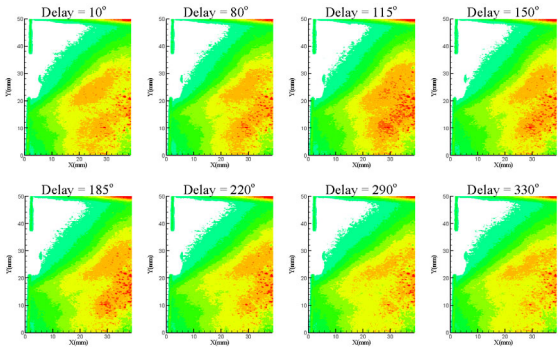

Figure 9 Partially premixed stable flame

When looking at correlations between pressure and heat release in case of good and bad control, one can get a better insight of how the control is effective by reducing correlations between heat and pressure oscillations. The example chosen is the one corresponding to Figure 7 and Figure 9. The point of measurement of CH* is perpendicular to the pressure probe. One can see in Figure 10 that for a bad control case, the heat release has a similar pattern than the pressure signals. Maximum intensity measured is 2.5, whereas the minimum is 0.6. For a good control, one can notice that the heat release is seems to be more uniform in time even though the influence of the pressure oscillations can be seen at some time. This is also the reason why a peak in the spectrum can still be detected, even in case of good control. The secondary injection is injected at the proper time delay to have a more uniform heat release during one cycle of oscillation. As shown in Figure 10, the instability period is about 5ms, showing that the oscillating frequency is of the order of 200Hz.

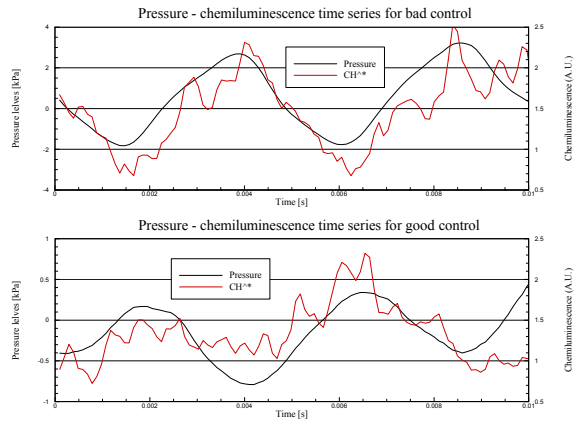

Figure 10 Pressure and CH* for good/bad control

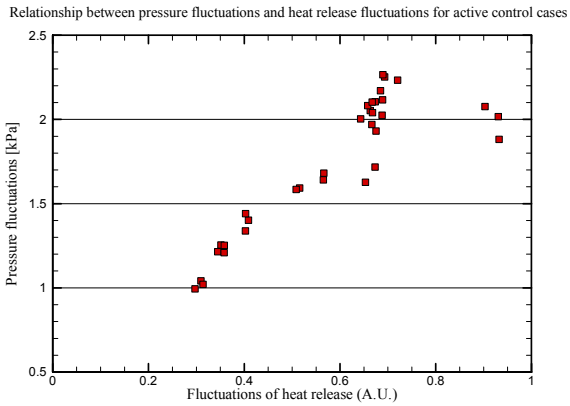

Figure 11 Relationship between heat release and pressure fluctuations

To emphasize more the relation between the fact that a good control is obtained for both reduced pressure and heat release fluctuations, the typical standard deviations are computed for cases where active control was successful and for case where it failed. The results for 33 different control output (delay and open time only were changed) are plotted in Figure 11, where the correlation between heat release fluctuations and pressure fluctuations is obvious. One can note however, that pressure oscillations seem to reach a maximum value around 2.2kPa, whereas heat release fluctuations do not present such apparent maximum.

The fact that heat release fluctuations continue to increase whereas pressure fluctuations seem to have a maximum value around 2.2kPa (limit cycle amplitude) comes from the fact that even though the heat release has a temporal signal close to the pressure one, is still deviates slightly as not presenting a perfect sine shape. The increase in the heat oscillations is coming from a shape in the heat release signal becoming more sinusoidal, being closer to the shape of the pressure signal. As the signal becomes sinusoidal, the fluctuations increase. The case presented in Figure 10 as bad control was obtained for pressure fluctuations of 2kPa and heat release fluctuations of 0.64, whereas the good control corresponds to 1.04kPa and 0.31 respectively.

4. Chemiluminescence for detecting precursors of thermo-acoustics oscillations

For active control strategies, it is very important to have sensors that can give in a very short time the appearance of self-sustained oscillations. Pressure signals is of course very efficient for this target, but the increase of pressure fluctuations are the results of the oscillations, not the cause. As known, it is the fact that heat release and pressure fluctuations are in phase that will provide energy to the oscillations, hence re-enforcing them and increasing the levels of pressure, which will in turn increase the levels of energy. Therefore, it seems more appropriate to try to measure the concordance of heat release rate versus pressure fluctuations with a good temporal resolution. The true Rayleigh index definition is the integral over one cycle and for the complete volume of pressure fluctuations times heat release fluctuations. This term is not easily obtained experimentally. Therefore, a slightly different expression is used in the following of this article. Computing a mean Rayleigh index (sum of pressure fluctuations times heat release fluctuations over 1 second along the volume of the lens integration), one can see a strong relation between this mean value and the mean pressure fluctuation levels inside the combustor, as depicted by the graph represented in Figure 12. For clarity reason, the logarithmic value (base 10) of Rayleigh sum is plotted on the right side as a function of equivalence ratio. The pressure fluctuations are plotted as RMS values in kPa on the left side of the graph. One can clearly see that for low values of pressure levels, the computed Rayleigh sum is negligible. For pressure levels of 0.7 to 0.75 kPa (which corresponds to equivalence ratio of 0.65 and 0.66 respectively), one can notice an increase of the Rayleigh sum from 1 to 2 (which corresponds to one order of magnitude in absolute value).
Afterwards, for a stoichiometry of 0.67, one can see that the pressure fluctuations reached a level of 1.52 kPa (two times higher than for f = 0.66).
The Rayleigh sum increase again from 2 to 6.5. Hence, it seems possible to gain more information using the Rayleigh sum than only pressure fluctuations to see the possible appearance of acoustics oscillations. A small increase in pressure can result in high increase in correlation between pressure and heat release, which will lead to self-sustained oscillations.

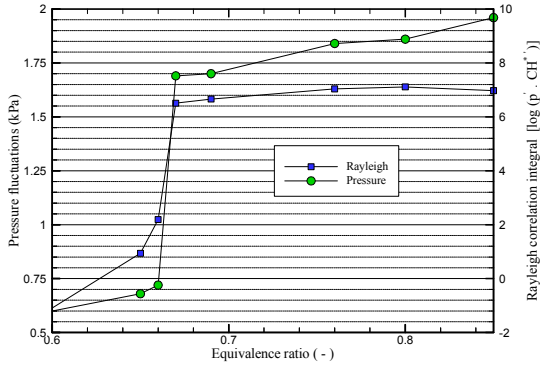

Figure 12 Relation between Rayleigh index and pressure fluctuations

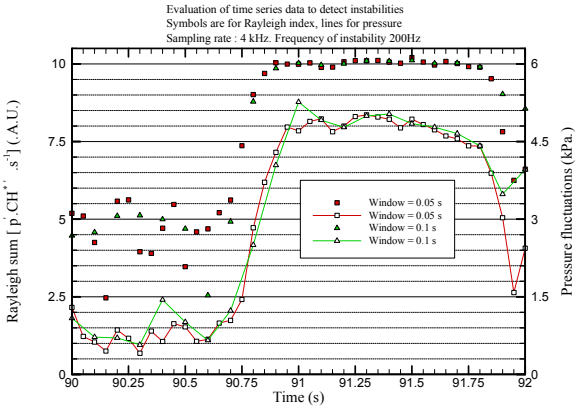

Figure 13 Time series Rayleigh index and pressure levels

The previous conclusion is valid for temporally stable situations. However, an important issue is the dynamics of the oscillations and to check if the Rayleigh information can provide faster results than just pressure levels considerations. Therefore, high sampling frequency is acquired and time-series measurements are analyzed to discuss this possibility. On Figure 13, a typical temporally resolved event is depicted (for which the origin of time is arbitrary chosen). The pressure fluctuations are displayed on the right axis in kPa and with open symbols, whereas the Log10 of the Rayleigh index is shown on the left axis with filled symbols. Two different integration times are considered, respectively 0.05 and 0.1s during which both pressure fluctuations and Rayleigh are computed. Therefore, there are twice more points for integration time of 0.05s (20Hz) rather than 0.1s (10Hz). One can notice that for time lower than 90.5s, the pressure fluctuations remain limited to levels lower than 1.5kPa, the Rayleigh index having values around 5. For a time of 90.75s, the Rayleigh index computed at 20Hz has a value of 7.5, which, as the scale is logarithmic constitutes a huge difference compared to previous levels around 5. On the opposite, for the same time, the pressure levels remain limited to 1.5kPa, which level was already reached before without leading to a sudden increase of the pressure levels inside the combustor. The next pressure sample rises to 3kPa whereas Rayleigh index rises to 9. This is clearly the appearance of strong self-induced oscillations, as previously reported in Figure 12. Through this example, it has been shown that using Rayleigh index as criteria for precursors of strong oscillations may result in a temporal gain of 0.05s, corresponding to 10 cycles. The reason for the emergence of an increase in the Rayleigh index is that heat release is phase-locked with pressure fluctuations prior to the increase of pressure levels. Therefore, for active controls strategies, one should also include a monitoring of the Rayleigh index. The decision to activate the active control may results in threshold on either pressure or Rayleigh levels. The actual transition will highly depend on the receiving optics of chemiluminescence (lens, fiber, photo-multiplies), so no general rule should

be educed from the present experiments as far as levels are concerned.

5. Chemiluminescence for designing active control loop

5.1. Dynamic calibration of actuators

An important aspect of chemiluminescence measurement is that it allows temporally resolved diagnostics of combustion. It is therefore a very useful tool to evaluate transient combustion process. In an active control loop, one important aspect is the actuator response time and its influence on the main combustion. If detailed knowledge are known concerning the actual combustion and duration of the secondary injections system, it is afterwards easier to model the action of the actuator and to predict the best performances prior to real testing where pressure levels may be very important, limiting the number of trials.
The first aspect is to measure accurately the time lag between the command of the actuator and its real effect on combustion. For this purpose, the signal of the valve is changed from frequency of 250Hz to a frequency of 260Hz. Recording both the command signal and the chemiluminescence signal allows a precise determination of the time lag between command and actual influence on combustion. The tests performed showed an actual time lag of 72ms.
The next aspect is to quantify the shape of the burning fuel injected as function of both frequency and duration time of valve opening. It has been shown that control may be achieved even using sub-harmonic injection (Lubarsky *et al.*, 2003). One of the main reasons is that typical gaseous actuators have a better response for lower frequency and therefore the injection of gas is better controlled, providing a better shape for the heat release. Chemiluminescent measurements were done, recording the time series heat release due to secondary injection system. The bulk velocity was set to 13 $m.s^{-1}$, the total equivalence ratio at 0.52 with a secondary injection percentage of 22.2%.

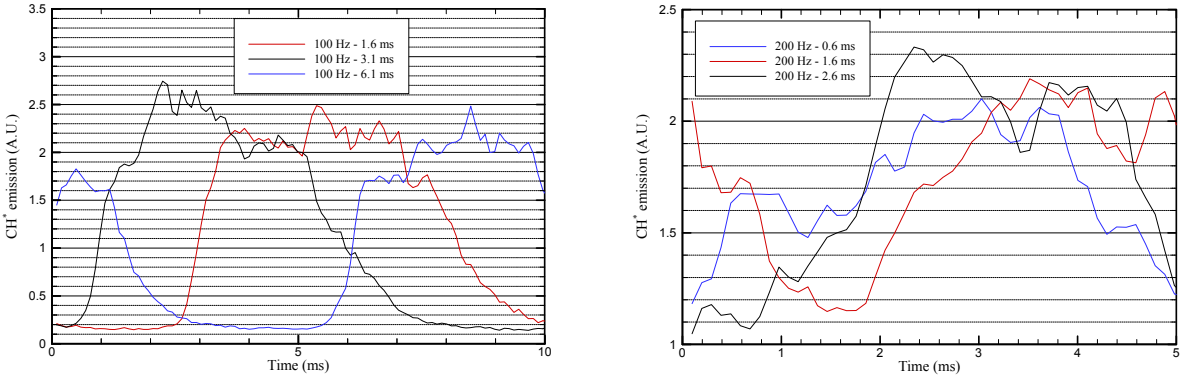

Figure 14 Real characteristics of secondary injection

Typical frequencies were ranging from 40 to 400 Hz whereas opening time was set at its lowest at 0.6 ms and the maximum depending on actuating frequency. CH* emission was recorded during the cycles of injection and the mean trace over 10 seconds are displayed on Figure 14 as function of both frequency and open time.
Different kind of signal can be sent to the actuator but in the following only step command (TTL) are investigated, providing a sharper signal than for instance a sinusoidal signal. One can notice that the traces obtained at lower frequencies are closer to a step than the one obtained at higher frequencies. One can also notice that the background emission is increasing with an increase of frequency, meaning the actual effects of the secondary injection are much smaller.

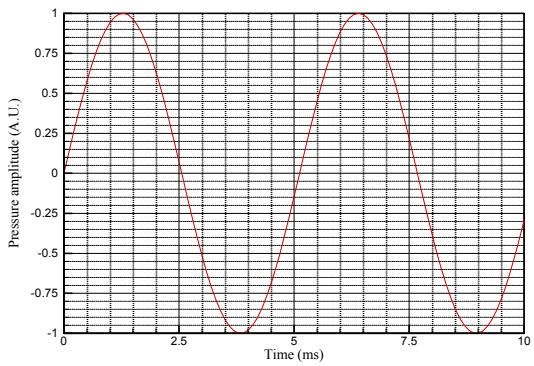

Figure 15 Theoretical pressure fluctuations

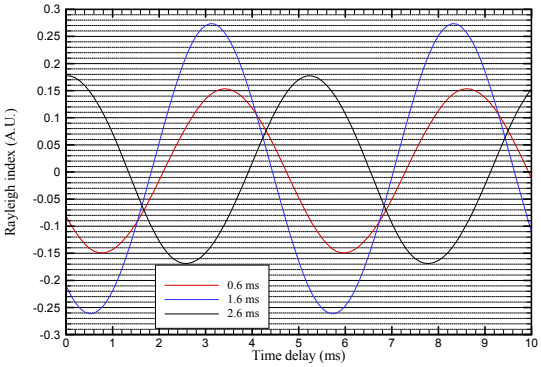

Figure 16 Theoretical Rayleigh estimation of the different configurations

This may come from the fact that the valve cannot completely be closed during one cycle and the percentage of fuel continuously injected becomes non-negligible. Having traces of heat release and the typical time lag between the command and the detection of the effect induced by the injection, it is possible to predict the effect of secondary injection on damping (or increasing) oscillations. Simulations are done by assuming a perfect sinusoidal signal for the pressure fluctuations, as shown in Figure 15 having only one frequency.
This approach is similar to the one adopted in (Lee and Santavicca, 2003). However, one of the main changes is that different frequencies for the valve are simulated to check a priori the best configuration possible. For each condition, a Rayleigh index may be computed assuming that there is a linear dependency between CH* and heat release. This is simply done by integrating the pressure fluctuations and the heat release fluctuations over one cycle. Typical results obtained are summarized in Figure 16 when simulating instability at 200Hz and controlling it with a secondary injection pulsing at 200Hz also. Three different valve opening times are compared (0.6; 1.6 and 2.6ms) and the Rayleigh index is computed.

5.2. Predicting control results

The lowest values are obtained for an opening time of 1.6ms at a time delay of 0.5ms after a positive slope in the pressure signal is detected. It is also important to notice that a bad phase delay will re-enforce the actual instabilities, as a positive Rayleigh index is computed for instance for the same opening command but with a delay of 3ms. This means that at least two variables (time delay and opening command) have to be optimized simultaneously to damp oscillations. In practice, there may be another factor to adjust: the actual frequency of the valve. In theory, the optimal frequency of control is the frequency of oscillations. However, for high frequencies instabilities, it may be possible that lower actuating frequencies will damp more the oscillations. Simulations for a frequency of 200Hz are displayed in Figure 17 for control frequency of 200 and 100Hz respectively. In this case, the best time delay between pressure and heat release is chosen and the results are only plotted with respect to opening time and frequencies of valve. One can see that the best damping performance is obtained for an injection of 200Hz whereas lower harmonics such as 100Hz still shows good results. It is worth noting that using very low injection would allow damping only one third as compared with harmonic injection for this specific case. Therefore, as long as the shape can be well controlled, one should use harmonic injection for active control strategies. The best results of the model for a thermo-acoustic instability with a frequency of 200Hz are hence obtained for a harmonic injection with an opening command of 1.6ms and a time delay around 0.5ms between the positive slope of the pressure and the TTL sending command. The next section shows actual comparison between the predictions and measurements performed in the demonstration combustor.

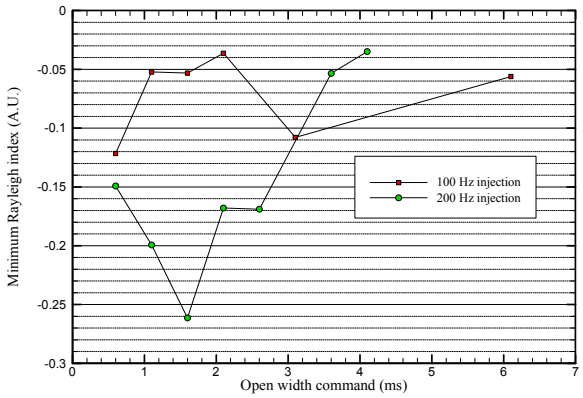

Figure 17 Predicted reductions acoustics oscillations

5.3. Comparisons with experiments

To validate the model, experiments are carried out. The inlet velocity is set to 12m.s^{-1}; the inlet temperature to 500K and the length of the combustor is 810mm. The percentage of secondary fuel was set to 14.25% and the total equivalence ratio was 0.88. To validate the model, the time delay as well as open width command is varied and pressure signals are measured. The typical frequencies measured are 220Hz, so the valve is operated at the same frequency. The first tests deal with the influence of time delay for a command of 1.6ms. The delay is varied from 0 to 3ms. The pressure amplitudes without control were 2.54kPa for an overall equivalence ratio of 0.85 and 0.90. The results are presented in Figure 18 where the modeled Rayleigh index is shown in the right side of the graph and the measured pressure fluctuations levels are shown on the left side. It is important to note that this Rayleigh index is the one coming from the secondary injection only and therefore should not be compared with previously reported values (Figure 12). One can notice that both data show a minimum for a delay around 0.5ms and then increase for higher and shorter delays. The fact that the two curves do not perfectly overlap may come from the fact that the frequency of the model was 200Hz and the real one 220Hz. The second reason is that the calibration of the valve were not performed exactly at the same condition of mass flow rate (hence velocity of secondary injection). However, the general behavior is obtained through the previously exposed model. Another series of tests consist in determining the best open width command for a fixed delay with respect to pressure signal. The results are shown in Figure 19, where the delay with respect to pressure is fixed at 0.4ms. The open command is changed from 0.6 to 2.1ms in the experiments and to 3.6 in the modeled data.

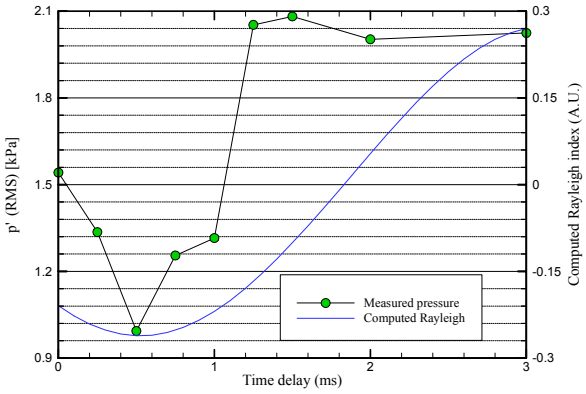

Figure 18 Time delay influence for open = 1.6ms

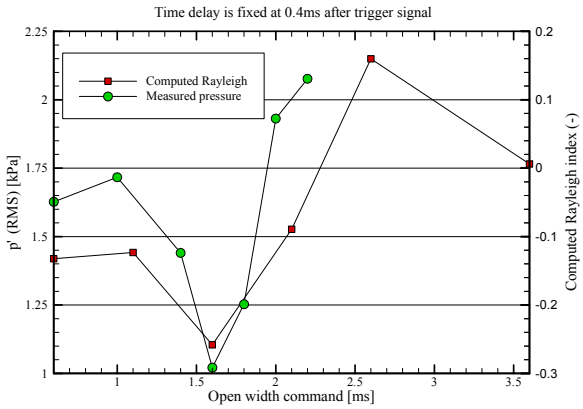

Figure 19 Open width command with delay=0.4ms

One can again notice that similar trends are found on both the experimental results and the results obtained though the model. The optimum point obtained experimentally corresponds to the predicted one. Hence, it seems possible to take benefit of the validity of the model to predict the behavior of the active control loop. It may result in initial conditions close to the optimum one and therefore be a good start for an active control loop with adaptive output to match time varying inputs.
Therefore, the model and the chemiluminescent measurements required as input are good tools for active control strategies, especially concerning the development of algorithm.

6. Conclusions

Chemiluminescent measurements have been used at different stages for building an active control loop of combustion oscillations. Taking the ratio of two wavelengths enabled measuring on-line the stoichiometry. The uncertainties reported were below 5% for a frequency of 10Hz. High data rate, joint with pressure measurements enabled a dynamic determination of the acoustic modes of the oscillations and criteria in terms of correlation between pressure and chemiluminescent emission fluctuations may be found to predict self-sustained oscillations. Phase-locked images of OH* showed that in case of oscillations, the flame shape is deformed by a vortex-like structure, issued from the inlet boundaries, which does not appear for stable combustion cases. Finally, time resolved chemiluminescent enabled to define the actual role of the secondary fuel injection. Strategies concerning frequency, amplitude and time delays of the actuators can be predicted using time lag assumption coupled to those measurements. This may limit the trials during active control loop as a priori a good set of parameters may be inferred from an existing database.
The next steps consist in combining to the simultaneous measurements of pressure and chemiluminescence, planar velocity to understand the actual dynamics of the flame and the possible modification induced by the secondary injection on the mean velocity profile and turbulence levels.

8. References

Anthoine, J., Mettenleiter, M., Repellin, O., Buchlin, J. -M., and Candel, S., *J. Sound Vib.* 262:1009-1046 (2003).
Docquier, N., Lacas, F., and Candel, S., *Proc. Combust. Inst.* 29:139–145 (2002).
Lee, J.G., Kim, K., and Santavicca, D. A., *Proc. Combust. Inst.* 28:415–421 (2000).
Lee, J.G., and Santavicca, D.A., *J. Prop. Power* 19:735-750 (2003).
Lubarsky, E., Shcherbik, D., Bibik, A., and Zinn, B.T., AIAA paper 2003-3180, 9th AIAA/CEAS Aeroacoustics Conference and Exhibit, South Carolina, 12-14 May (2003).
Muruganandam, T.M., Kim, B., Olsen, R., Patel, M., Romig, B., and Seitzman, J.M., AIAA paper 2003-4490, 39th AIAA/ASME/SAE/ASEE Joint propulsion Conference and Exhibit, Hunstville, Alabama, July 20-23 (2003).
Sanders, S. T., Mattison, D. W., Jeffries, J. B., and Hanson, R. K. *Proc. Combust. Inst.* 29:2661–2667 (2002).
Tachibana, S., Zimmer, L., Yamamoto, T., Kurosawa, Y., Ysohida, S., and Suzuki, K., in Proceedings of the 5th symposium on smart control of turbulence, Tokyo, February (2004).
Taupin, B., Vauchelles, D, Cabot, G, and Boukhalfa, A. 11th International Symposium on Applications of Laser Techniques to Fluid Mechanics, 8-11 July, Lisbon (2002).
Wachsman, A., Park, S., Sobhani, Z.C., Annaswamy, A.N., and Ghoniem, A.F., AIAA paper 2004-0633, 42nd AIAA Aerospace Sciences Meeting and Exhibit, Reno, NV, Jan. (2004).
Zimmer, L., Tachibana, S., Yamamoto, T., Kurosawa, Y., and Suzuki, K., in Proceedings of the 4th symposium on smart control of turbulence, Tokyo, March 2-4, pp 93-102 (2003).